CHIN. PHYS. LETT. Vol. 37, No. 1 (2020) 017402 **Express Letter**

Observation of Coulomb Gap and Enhanced Superconducting Gap in Nano-Sized Pb Islands Grown on $SrTiO_3$ *

Yonghao Yuan(袁永浩)[1,2], Xintong Wang(王心童)[1,2], Canli Song(宋灿立)[1,2], Lili Wang(王立莉)[1,2], Ke He(何珂)[1,2], Xucun Ma(马旭村)[1,2], Hong Yao(姚宏)[1,2,3], Wei Li(李渭)[1,2**], Qi-Kun Xue(薛其坤)[1,2,4**]

[1]*State Key Laboratory of Low-Dimensional Quantum Physics, Department of Physics, Tsinghua University, Beijing 100084*

[2]*Frontier Science Center for Quantum Information, Beijing 100084*

[3]*Institute for Advanced Study, Tsinghua University, Beijing 100084*

[4]*Beijing Academy of Quantum Information Sciences, Beijing 100193*

(Received 10 December 2019)

We report high-resolution scanning tunneling microscopy (STM) study of nano-sized Pb islands grown on $SrTiO_3$, where three distinct types of gaps with different energy scales are revealed. At low temperature, we find that the superconducting gap (Δ_s) in nano-sized Pb islands is significantly enhanced from the one in bulk Pb, while there is no essential change in superconducting transition temperature T_c, giving rise to a larger BCS ratio $2\Delta_s/k_BT_c \sim 8.31$ and implying stronger electron-phonon coupling. The stronger coupling can originate from the interface electron-phonon interactions between Pb islands and $SrTiO_3$. As the superconducting gap is totally suppressed under applied magnetic field, the Coulomb gap with apparent V-shape emerges. Moreover, the size of Coulomb gap (Δ_C) depends on the lateral size of Pb islands (R) with $\Delta_C \sim 1/R^{0.35}$, indicating that quantum size effect can significantly influence electronic correlations. Our experimental results shall shed important light on the interplay among superconductivity, quantum size effect and correlations in nano-sized strong-coupling superconductors.

PACS: 74.78.−w, 74.78.Na, 74.55.+v, 73.22.−f, 73.23.Hk DOI: 10.1088/0256-307X/37/1/017402

Electronic properties in quantum materials may be qualitatively modified by reducing their size and/or dimensions, which have attracted extensive interests in condensed matter physics research. One intriguing discovery in size confined systems is the enhancement of superconductivity in nano-sized weak coupling superconducting films, such as Al, In and Sn.[1,2] The mechanism of enhanced superconductivity has been explained as surface phonon softening,[3] which leads to the enhanced electron-phonon coupling based on Eliashberg theory.[4,5] In contrast, T_c of strong coupling superconductors, like Pb, is hardly boosted by reducing their size. Actually, in two-dimensional Pb films grown on Si(111), T_c shows oscillating decrease tendency with the decreasing film thickness.[6,7] To obtain enhanced surface phonon coupling, Pb nanoparticles with higher surface-area ratio are prepared, in which the T_c presents a constant value (still lower than that of bulk Pb) with the size reduction until approaching the Anderson limit.[8,9]

When their sizes are smaller than the Anderson limit (∼10 nm), both the weak and strong coupling superconductors lose their superconductivity.[10] In this zero-dimensional limit, extreme electronic correlation dominates and induces Coulomb blockade phenomenon. Indeed, studies on nano-sized silver particles[11] and graphene nano-ribbons[12] have shown that Coulomb interaction is significantly enhanced during size reduction, which may even induce metal-insulator transition. Besides the electron-electron interaction, electron-phonon interaction is modified by size effect as well, manifesting as pseudogap feature observed in Pb islands.[13] Therefore, electronic properties of low-dimensional superconductors are more complicated than expected, and we need to revisit the influences of both Coulomb and electron-phonon interactions in those systems.

It has been experimentally established that superconductivity can be significantly enhanced in a monolayer FeSe film grown on $SrTiO_3$,[14] demonstrating that metal-oxide interface could be another key factor to boost T_c.[14−16] Hence, by constructing a new system that can combine all those factors together, it would provide an ideal platform to study their interplay with two-dimensional superconductivity.

In this Letter, we report on molecular beam epitaxy (MBE) growth and systematic STM studies of laterally confined Pb islands on $SrTiO_3$(001) (Pb/STO). Three distinct types of energy gaps have been observed, which are the superconducting gap, Coulomb gap, and pseudogap. They manifest themselves in different energy scales. At low temperature, the superconducting gap in Pb/STO is enlarged, with the gap size (Δ_s) of ∼2.50 meV, larger than 1.36 meV

*Supported by the National Natural Science Foundation under Grant Nos. 11674191 and 11825404, the National Key Program for S&T Research and Development under Grant No. 2016YFA0301002, and the Beijing Advanced Innovation Center for Future Chip (ICFC). W.L. was also supported by Beijing Young Talents Plan.

**Corresponding authors. Email: weili83@tsinghua.edu.cn; qkxue@mail.tsinghua.edu.cn

© 2020 Chinese Physical Society and IOP Publishing Ltd

for bulk Pb. However, the T_c in Pb/STO is not enhanced from the bulk value, giving rise to a larger BCS ratio $2\Delta_s/k_BT_c \sim 8.31$ in the nano-sized Pb/STO. When the superconductivity is suppressed under applied magnetic field, Coulomb gap ($\Delta_C \sim 1$ meV) induced by electronic interaction is clearly revealed. The value of Coulomb gap increases with reduction of the lateral size of Pb islands. As the lateral size approaches the Anderson limit, Coulomb blockade feature starts to appear. Finally, a pseudogap Δ_p with the magnitude of ~ 10 meV, at rather larger energy scale, is visible (even at 30 K), which may originate from the weakening of electron-phonon interaction.[13]

Figure 1(a) shows a typical STM topographic image of Pb islands grown on the $SrTiO_3$ (STO) substrate. The atomic resolution result (see Section 1 in the Supplementary Material) shows hexagonal lattice with lattice constant of 3.49 Å on Pb islands, in good agreement with that of the (111) surface of FCC-phase Pb. The lattice constant of STO is 3.9 Å. Due to the large lattice mismatch as well as the decomposed surface oxygen of STO during the Pb growth, the growth follows the Stranski–Krastanov mode (i.e., islands start to form after the growth of a wetting layer of Pb) and the wetting layer is much rougher than that of Pb grown on Si (111). Three types of Pb islands classified as A, B and C are obtained. The type-A islands are thicker than 15 nm, and exhibit the superconducting gap similar to that of bulk Pb (see Fig. 1(b)). The U-shaped superconducting gap is fitted well by the Dynes model,[17] and the fitted gap value is 1.36 meV with scattering rate $\Gamma_A \sim 0.08$ meV, consistent with that of its bulk material.

The heights of type-B Pb islands are 3–8 nm and their areas range from 1000 nm^2 to 100000 nm^2. The dI/dV spectrum shows a larger superconducting gap but with lower coherence peaks (Fig. 1(c)). The fitting result suggests that the magnitude of the enlarged superconducting gap Δ_s is 2.58 meV and the corresponding scattering rate Γ_B is 0.24 meV. Systematic study on the enlarged superconducting gap is shown in Section 2 in the Supplementary Material. The well-defined superconducting gap enlargement of Pb has not been reported yet, and we attribute the origin of the gap enhancement here to the special substrate (STO) used. The STO-Pb interface may provide additional electron-phonon coupling channel to enhance the superconducting pairing strength. The fitting curve deviates from the data at the bottom of the gap near the Fermi level (E_F), implying the existence of non-BCS behaviors in the type-B islands. Type-C islands are of the smallest size, usually smaller than 500 nm^2. The dI/dV spectrum (Fig. 1(d)) shows several discrete peaks, which are signatures for Coulomb blockade.[18] The Coulomb blockade can be observed here owing to the imperfect interface between STO and Pb. Meanwhile, superconductivity here is absent due to approaching of the Anderson limit.[10] Since type-B islands present the most intriguing electronic properties, we mainly focus on this type of Pb islands in our following discussion.

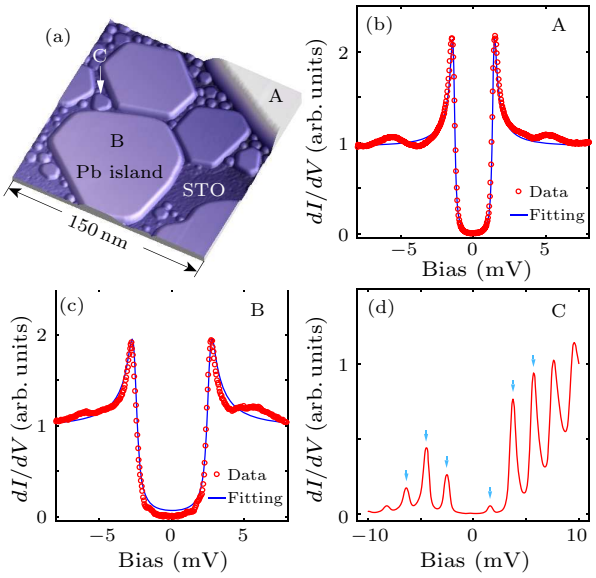

Fig. 1. (a) STM topographic image of Pb islands grown on the STO(001) substrate (150 nm ×150 nm. Set point: bias voltage $V_s = 2.0$ V, tunneling current $I_t = 20$ pA). [(b), (c)] The dI/dV spectra taken on type-A and type-B Pb islands grown on STO substrates, respectively (400 mK, $V_s = 10$ mV, $I_t = 400$ pA). The data are presented with red circles, and the fitting results by the Dynes model are in blue curves. Type-A islands behave like bulk Pb and show a 1.36-meV superconducting gap. Type-B islands show an enlarged 2.58-meV gap. (d) The dI/dV spectra taken on a type-C Pb island (400 mK, $V_s = 10$ mV, $I_t = 400$ pA). The discrete peaks, denoted by cyan arrows, are signatures of Coulomb blockade.

Superconducting gaps of type-B Pb islands are strongly suppressed by externally applied magnetic field. Figure 2(a) exhibits the dI/dV spectra taken on an island with applying various perpendicular magnetic fields. The effective radius (R) of the island is ~32.8 nm, where R is estimated by the formula $R = (\text{area}/\pi)^{1/2}$. The superconducting gap keeps shrinking with increasing applied magnetic fields and persists even up to 0.75 T, indicating an enhancement of upper critical field of the Pb islands compared with its bulk value ~0.08 T. Remarkably, the gap feature is no longer sensitive to magnetic field from 1.5 T and such a residual gap is unchanged up to 15 T. The magnitude of this field insensitive gap Δ_C is ~0.65 meV (see Fig. 2(a) and Fig. S3).

The residual gaps are V-shaped (see Figs. 2(a) and 2(b)) and the density of states (DOS) exhibits a linear dependence on energy near E_F (see Figs. S3 and S4). Theoretical work has proposed that in two-dimensional correlated systems, Coulomb gap may develop and the DOS of corresponding electrons near E_F linearly depend on energy: $G \sim |E|$.[19] Therefore, the residual gap here may be Coulomb gap induced by electronic correlation. Previous studies on

Coulomb gap mainly focused on amorphous metals[20] and doped semimetals,[21] in which variable range hopping of localized electrons with poor screening dominates the conductivity. By reducing the size of a Pb island to cross from two-dimensional to zero-dimensional limit, Coulomb gap becomes pronounced for the following reasons: (i) Coulomb interaction affects in longer range according to the Lindhard screening theory.[22] (ii) The itinerant s-electrons have spill-out effect, which further weakens the screening effect on smaller islands.[23] When the values of Δ_C and Δ_s are comparable in a low-dimensional system, another interesting phenomenon is the possible change of effective charge of a single electron, which still requires further investigations.[24]

To investigate the relationship between the Coulomb gap and the size of Pb islands, a series of dI/dV spectra (Fig. 2(b)) are taken on various Pb islands. High magnetic fields are applied to suppress the superconducting gap and highlight the Coulomb gap. As is expected, Δ_C becomes larger and deeper as R decreases, showing that Coulomb interaction is indeed affected by size effect and is more pronounced in smaller islands. Based on the fitting of our results, the Coulomb gap size (Δ_C) has a power-law dependence on R: $\Delta_C \sim 1/R^{0.35}$. Δ_C and R are plotted out in logarithmic scales in Fig. 2(c), where the exponent 0.353 is obtained from the slope of the fitting curve. Similarly, as shown in Fig. 2(d), the logarithmic zero energy density of states (G_0) obeys $\ln G_0 \sim -1/R^{1.91}$, where the exponent 1.91 is very close to 2, indicating G_0 decays exponentially with 1/area. It is noteworthy that the spectrum on a small island with $R = 23.1$ nm shows a harder gap and several peak feature (denoted by cyan arrows in Fig. 2(b)) outside the gap, indicating that the system approaches Coulomb blockade regime (like type-C islands) as the lateral size of island keeps decreasing. Pb islands were grown on $SrTiO_3$ substrates with different Nb doping levels (0.7%, 0.25% and 0.15%), while the data taken on those substrates obey the same fitting curve (see the data points with different color in Fig. 2(b)–2(d)), demonstrating that the Coulomb gap is not sensitive to the details of substrates as well as their interfaces. We note that a previous study has also found an area-dependent gap feature on Pb islands and explained it as dynamic Coulomb blockade phenomenon.[25] However, superconductivity of Pb is absent in that work, presenting a sharp distinction from our system.

We further studied magnetic field response on a larger type-B island ($R \sim 83.7$ nm). Since the Bean–Livingston barrier[26] is overcome, a magnetic vortex is observed. Figure 3(a) shows the zero-bias dI/dV maps taken under different magnetic fields. The vortex emerges at 0.18 T and becomes blurred at 0.27 T. A linear fit on the extracted zero bias conductance values away from the vortex suggests an upper critical field ($\mu_0 H_{c2}$) of 0.30 T (see Fig. S5). H_{c2} is determined by the G-L coherence length ξ_{GL}: $\mu_0 H_{c2} = \Phi_0/2\pi\xi_{GL}^2$, where Φ_0 is magnetic flux quanta. Accordingly, the calculated coherence length ξ_{GL} is 33 nm, smaller than that of bulk Pb value (83 nm). A series of dI/dV spectra are taken across a vortex at 0.20 T and shown in Fig. 3(b). In the vortex core, a zero-bias peak originating from the Caroli-de Gennes-Matricon bound states is clearly revealed, indicating that this two-dimensional superconducting system is in clean limit. In contrast, the superconducting Pb islands grown on Si (111) are always in dirty limit, and the bound states are absent in the vortex core.[27]

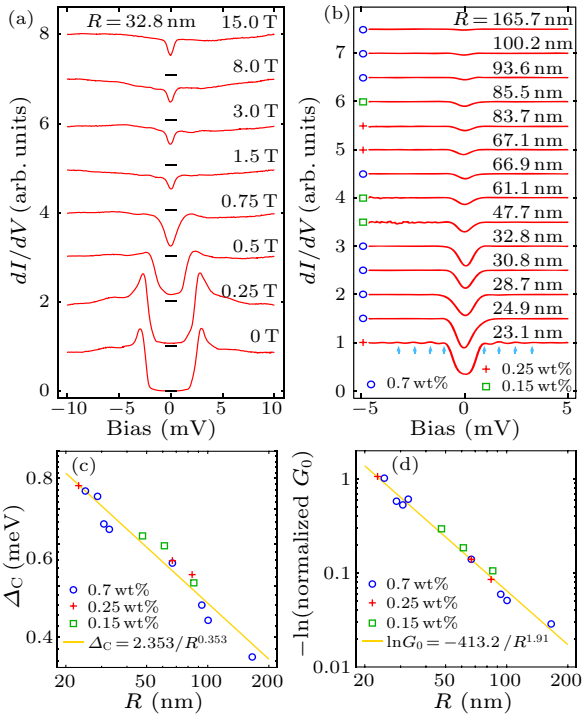

Fig. 2. (a) The dI/dV spectra taken on type-B Pb islands ($R = 32.8$ nm) under various magnetic fields (400 mK, $V_s = 10$ mV, $I_t = 300$ pA). Upper critical field is enhanced, compared with that of bulk Pb. A residual gap still exists at high fields as superconductivity is totally suppressed. The magnetic insensitive residual gap is attributed to the Coulomb gap. (b) Coulomb gaps of Pb islands with different areas (for details, see Section 3 in the Supplementary Material). The blue circles, red crosses and green squares denote 0.7 wt%, 0.25 wt% and 0.15 wt% Nb-doped substrates, respectively. The cyan arrows denote the Coulomb blockade features. (c) Double logarithmic scale plot of Coulomb gap size and lateral size of Pb island. The fitting result suggests $\Delta_C = 2.353/R^{0.35}$. (d) Double logarithmic scale plot of negative logarithmic zero-energy density of states ($-\ln G_0$) and lateral size of Pb island. G_0 exponentially decays with 1/area, which obeys $G_0 = \exp(-413.2/R^{1.9})$.

Our temperature-dependent measurements show that the superconducting gap is almost filled at 7.0 K (Fig. 3(c)). The fitting result suggests that the T_c is not higher than 7.3 K (see Fig. S6), which does not show significant enhancement compared with the T_c of bulk Pb. Intriguingly, the unchanged T_c associated with the enlarged superconducting gap Δ_s leads

to a rather large BCS ratio $(2\Delta_s/k_BT_c) \sim 8.31$, close to the ratio in cuprates.[28] The enlarged BCS ratio indicates that Pb, an inherent strong coupling superconductor, becomes even more strong-coupled when grown on STO. The theoretical work has pointed out that the BCS ratio may be increased through the mechanism of surface phonon softening.[29] In our case, electron-phonon coupling on metal-oxide interface provides another possible channel to enhance the coupling strength.

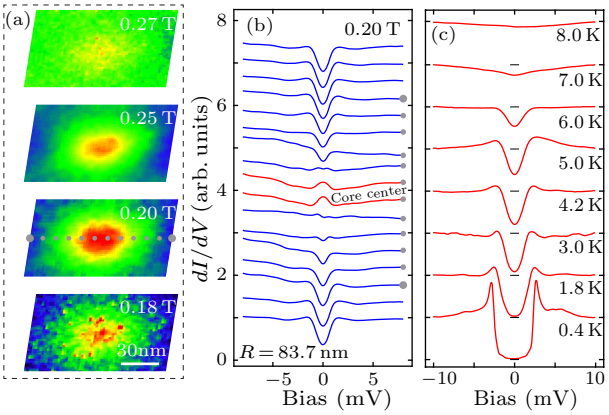

Fig. 3. (a) Zero-bias dI/dV maps taken on an $R \sim 83.7$ nm island under different magnetic fields. The red color region, corresponding to higher conductance area, indicates the suppression of the superconducting gap and emergence of a vortex. (b) A series of dI/dV spectra taken across the vortex at 0.20 T (the corresponding positions are denoted by a grey dotted line in (a), $V_s = 10$ mV, $I_t = 200$ pA). A zero-bias peak is observed in the vortex core. (c) The dI/dV spectra taken on an $R = 30.8$ nm Pb island at various temperatures ($V_s = 10$ mV, $I_t = 200$ pA). The superconducting gap is almost suppressed at 7.0 K, which does not show significant enhancement compared with that of bulk Pb.

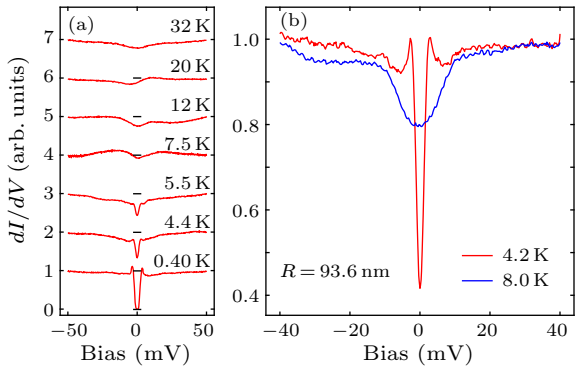

Fig. 4. (a) Larger-energy-range dI/dV spectra taken on an $R \sim 100$ nm Pb island at various temperatures ($V_s = 50$ mV, $I_t = 200$ pA). When temperature is higher than T_c, a pseudogap persists near E_F. (b) Large range dI/dV spectra taken on an $R = 93.6$ nm island ($V_s = 50$ mV, $I_t = 200$ pA). The red and blue curves show the spectra taken at 4.2 K and 8.0 K, respectively. The pseudogap coexists with the superconducting gap below T_c, as shown by the red curve.

Normal state of Pb islands is further investigated by larger energy range dI/dV spectra. As shown in Fig. 4(a), a larger gap Δ_p with magnitude of ~10 meV is observed above T_c and even exists at 32 K. This pseudogap feature has already been studied in the Pb/Si system, explained as a modification to Fabry–Pérot mode due to the weakening of electron-phonon interaction below Debye energy.[13] A previous study on TiN has also found a pseudogap above T_c, which was explained as superconducting fluctuations.[30] According to our data, the pseudogap not only shows up above the T_c, but also coexists with the superconducting gap (see the dip features outside the superconducting gap in Fig. 4(b)). Therefore, the origin for the pseudogap observed in our study is probably not the superconducting fluctuation.

We have found that the superconducting pairing strength is significantly enhanced by STO substrate. The extra electron-phonon coupling channel on the Pb/STO interface is a possible explanation for the enhancement. However, the Coulomb interaction competes with the effect and probably hinders the boost of T_c in two ways. On the one hand, the Coulomb repulsion directly competes with the formation of Cooper pairs. On the other hand, the drop of DOS near E_F induced by the Coulomb gap restricts the potential of T_c enhancement. We demonstrate that the quantum size effect plays an important role to influence electronic correlation, which was usually ignored in two-dimensional superconducting systems in previous studies. Our finding sheds new light on understanding the interplay among superconductivity, quantum size effect, and complex electronic properties in low-dimensional quantum systems.

Methods: Our experiments were conducted in a commercial ultra-high vacuum STM (Unisoku), which is connected to an MBE chamber for sample preparation. In the MBE chamber, Nb-doped STO substrates were pre-treated at 1200℃ to obtain TiO_2-terminated surfaces. High-purity Pb (99.999%) was thermally evaporated from a standard Knudsen cell at 450℃. During the sample growth, the substrate was kept at room temperature. Our STM measurement was carried out at a base temperature of 400 mK. Vertical magnetic field up to 15 T can be applied. The dI/dV spectra were measured using the standard lock-in method with 973.0 Hz bias modulations.

References

[1] Cohen R W and Abeles B 1968 *Phys. Rev.* **168** 444
[2] Bose S and Ayyub P 2014 *Rep. Prog. Phys.* **77** 116503
[3] Watson J H P 1970 *Phys. Rev. B* **2** 1282
[4] Eliashberg G 1960 *Sov. Phys.-JETP* **11** 696
[5] McMillan W 1968 *Phys. Rev.* **167** 331
[6] Guo Y et al 2004 *Science* **306** 1915
[7] Eom D et al 2006 *Phys. Rev. Lett.* **96** 027005
[8] Bose S et al 2009 *J. Phys.: Condens. Matter* **21** 205702
[9] Vlaic S et al 2017 *Nat. Commun.* **8** 14549
[10] Anderson P W 1959 *J. Phys. Chem. Solids* **11** 26
[11] Voisin C et al 2000 *Phys. Rev. Lett.* **85** 2200
[12] Han M Y et al 2007 *Phys. Rev. Lett.* **98** 206805
[13] Wang K et al 2009 *Phys. Rev. Lett.* **102** 076801

[14] Wang Q Y et al 2012 *Chin. Phys. Lett.* **29** 037402
[15] Ginzburg V L 1964 *Phys. Lett.* **13** 101
[16] Cohen M H and Douglass D H 1967 *Phys. Rev. Lett.* **19** 118
[17] Dynes R C et al 1978 *Phys. Rev. Lett.* **41** 1509
[18] Kastner M A 1992 *Rev. Mod. Phys.* **64** 849
[19] Efros A and Shklovskii B 1975 *J. Phys. C* **8** L49
[20] Butko V Y et al 2000 *Phys. Rev. Lett.* **84** 1543
[21] Massey J G and Lee M 1995 *Phys. Rev. Lett.* **75** 4266
[22] Lindhard J 1954 *K. Dan. Vidensk. Selsk. Mat. Fys. Medd.* **28** 8
[23] Liebsch A 1993 *Phys. Rev. B* **48** 11317
[24] Chen T et al 2012 *Phys. Rev. B* **86** 045135
[25] Brun C et al 2012 *Phys. Rev. Lett.* **108** 126802
[26] Bean C and Livingston J 1964 *Phys. Rev. Lett.* **12** 14
[27] Nishio T et al 2008 *Phys. Rev. Lett.* **101** 167001
[28] Fischer Ø et al 2007 *Rev. Mod. Phys.* **79** 353
[29] Leavens C R and Fenton E W 1981 *Phys. Rev. B* **24** 5086
[30] Sacepe B et al 2010 *Nat. Commun.* **1** 140
[31] Bose S et al 2010 *Nat. Mater.* **9** 550

Supplementary Material: Observation of Coulomb Gap and Enhanced Superconducting Gap in Nano-Sized Pb Islands Grown on $SrTiO_3$*

Yonghao Yuan(袁永浩)[1,2], Xintong Wang(王心童)[1,2], Canli Song(宋灿立)[1,2], Lili Wang(王立莉)[1,2], Ke He(何珂)[1,2], Xucun Ma(马旭村)[1,2], Hong Yao(姚宏)[1,2,3],

Wei Li(李渭)[1,2**], Qi-Kun Xue(薛其坤)[1,2,4**]

[1]*State Key Laboratory of Low-Dimensional Quantum Physics, Department of Physics, Tsinghua University, Beijing 100084*
[2]*Collaborative Innovation Center of Quantum Matter, Beijing 100084*
[3]*Institute for Advanced Study, Tsinghua University, Beijing 100084*
[4]*Beijing Academy of Quantum Information Sciences, Beijing 100193*

*Supported by the National Science Foundation (No. 11674191), Ministry of Science and Technology of China (No. 2016YFA0301002), and the Beijing Advanced Innovation Center for Future Chip (ICFC). W.L. was also supported by Beijing Young Talents Plan and the National Thousand-Young-Talents Program.

**Corresponding authors. Email: weili83@tsinghua.edu.cn; qkxue@mail.tsinghua.edu.cn

1. Lattice structure of Pb island

Figure S1 exhibits the atomic resolution image of Pb island grown on STO substrate. It presents a hexagonal lattice with lattice constant of 3.49 Å, consistent with that of the (111) surface of FCC phase Pb.

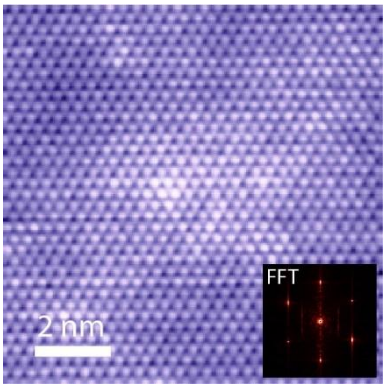

Figure S1. Atomic resolution of Pb island on STO. A STM image taken on a Pb island (set point voltage (V_s) = 45 mV, tunneling current (I_t) = 40 pA). It shows a hexagonal lattice with lattice constant of 3.49 Å.

2. The relationship between superconducting gap and Pb island size

Figure S2a-c show the dependence of superconducting gap on Pb island size. The superconducting gap size ranges from 2.2 meV to 2.8 meV, which may originate from the shell effect in nano-sized superconductors.[1] The gap size doesn't show significant dependence on island height (see Figure S2a). The gap size seems to decrease with island area

(Figure S2b), but the uncertainty of the gap size make it challenge to make a definite conclusion. The existence of the Coulomb gap, which is related with the island area, may have an affect the investigation as well.

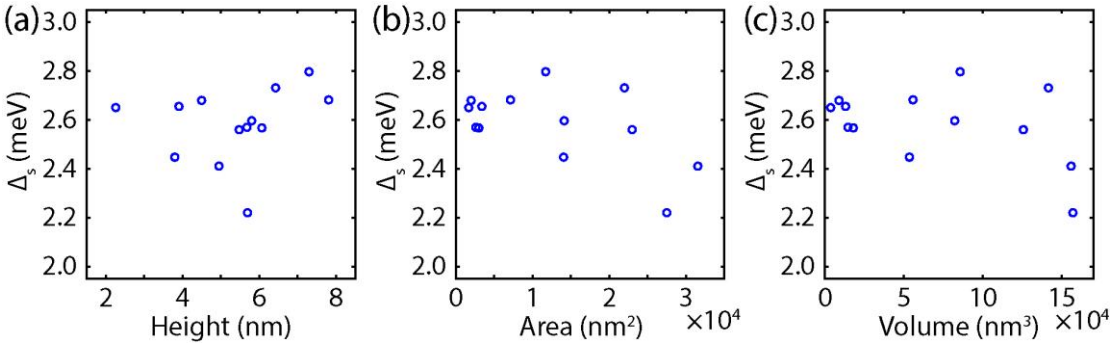

Figure S2. Dependence of superconducting gap on Pb island size. (a-c) The correlation between superconducting gap and Pb island height, area and volume, respectively.

3. Coulomb gap

Figure S3 shows the d*I*/d*V* spectra taken on different Pb islands, where their superconductivity is totally suppressed by applying high magnetic fields. Coulomb gaps are clearly revealed in these spectra but some of them also exhibit non-negligible background. In order to compare the zero-bias conductance (ZBC) and obtain the reliable gap sizes from these data, the d*I*/d*V* spectra are normalized. The background in each spectrum is simulated by a Bezier curve drawn from the data outside the gap energy (the red curves in Figure S3a1-n1). Then the background is divided from each spectrum and the normalized data are shown in Figure S3a2-n2. The ZBC values (G_0) are obtained from the normalized data.

As mentioned in the main text, the spectrum on the smallest island in Figure 2b shows a harder Coulomb gap and starts to present Coulomb blockade feature (also see Figure S3a2). The Coulomb gap width in this spectrum is determined by the lowest energy peaks denoted by green arrows in Figure S3a2. Except for this spectrum, the normalized spectra all show V-shaped gap feature, which is the signature for Coulomb gap. Density of states (DOS) in Coulomb gaps are linearly depend on energy and can be tracked well by linear fits (green lines in Figure S3b2-n2). The Coulomb gap width is determined by the bias voltage at which the value of the fitting function equals to 1.

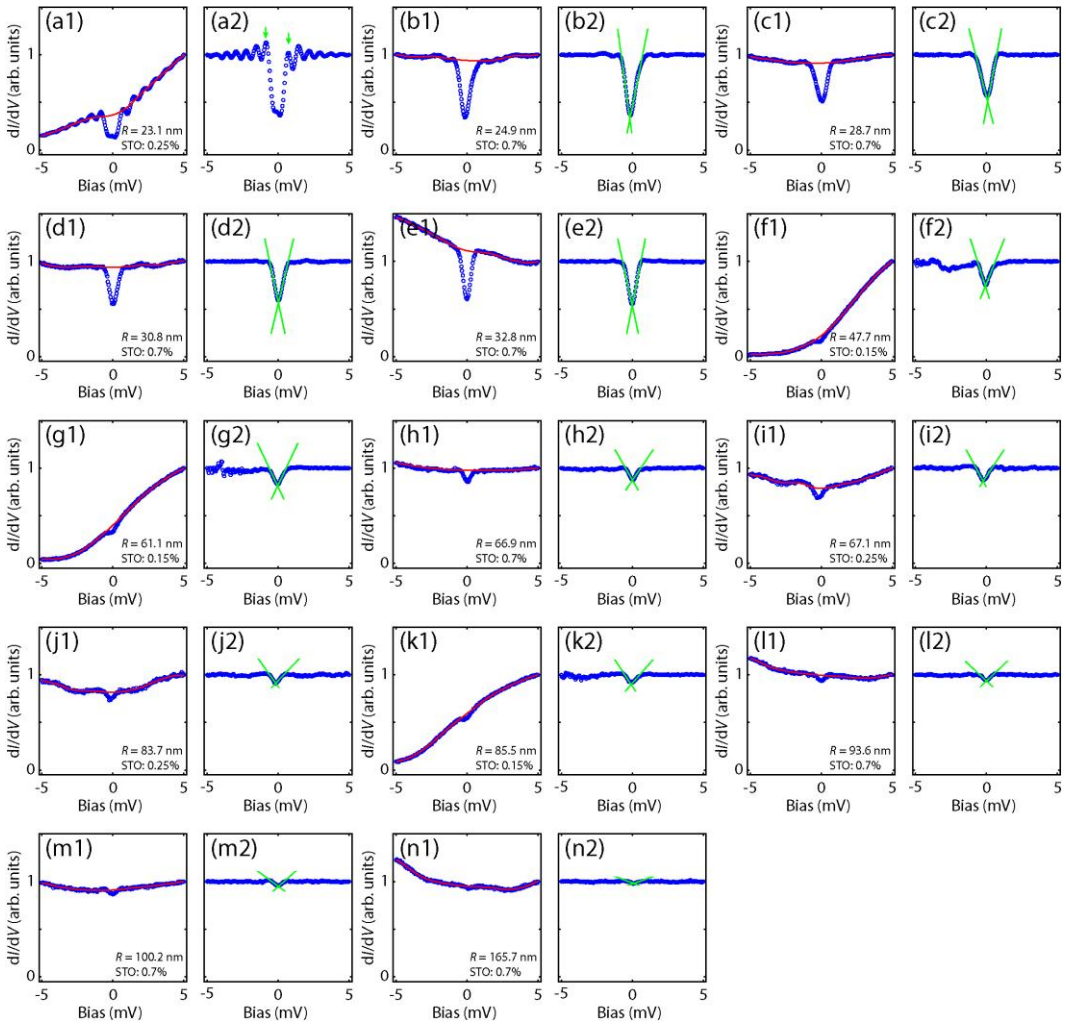

Figure S3. Normalization of dI/dV spectra and Coulomb gap. (a1-n1) dI/dV spectra taken on Pb islands with applying high magnetic fields (V_s = 10 mV, I_t = 200 pA). The blue circles and red curves denote the raw data and the background, respectively. (a2-n2) Normalized spectra. The green arrows in (a2) denote the lowest energy peaks. The green lines in (b2-n2) are the linear fitting lines for Coulomb gaps.

4. Linear dependence of DOS on energy inside Coulomb gap

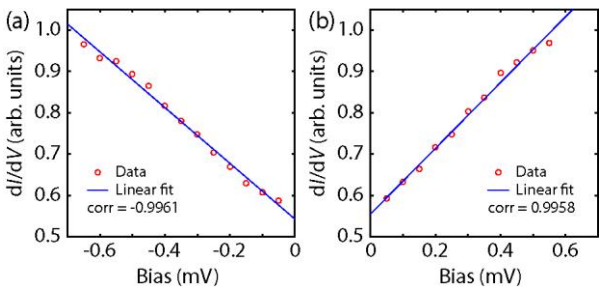

Figure S4. Linear dependence of DOS inside Coulomb gap. (a, b) Data points inside the Coulomb gap, which are extracted from the spectra in Figure S3d2. The DOS (G) and energy (E) show good linear relationship.

To demonstrate the linear increase of DOS in Coulomb gap, as an example, the in-gap data in Figure S3d2 are extracted and plotted in Figure S4. Correlation coefficients between DOS (G) and energy (E) are -0.9961 for negative bias and 0.9958 for positive bias. The absolute values are both very close to 1, indicating G is linearly depend on E. This result is consistent with Coulomb gap in two-dimensional systems whose DOS obeys: $G \sim |E|$.[2]

5. Upper critical field (H_{c2})

In the R = 83.7 nm Pb island, a vortex is observed under applied magnetic fields. The ZBC values taken away from the vortex are plotted in Figure S5 and the upper critical field is estimated by a linear fit. Due to the existence of Coulomb gap, the ZBC can't reach 1 even at very high fields. Therefore, the upper critical field should be corresponding to the ZBC value = the G_0 value in Coulomb gap (in this case, G_0 = 0.92). As shown in Figure S5, the corresponding upper critical field of this island is 0.30 T.

The upper critical field is sensitive to the size of Pb island, since H_{c2} is determined by G-L coherence length ξ_{GL}: $\mu_0 H_{c2} = \Phi_0/2\pi\xi_{GL}^2$. ξ_{GL} is monotonically increased with quasiparticle mean free path l. Taking the size effect into account, l approximately obeys: $1/l = 1/l_0 + 1/R$, where l_0 is the original mean free path. Therefore, the upper critical fields in smaller islands are expected to be higher than those in larger islands. The magnetic field response on a smaller island (R = 32.8 nm) indeed obey this law (mentioned in the main text).

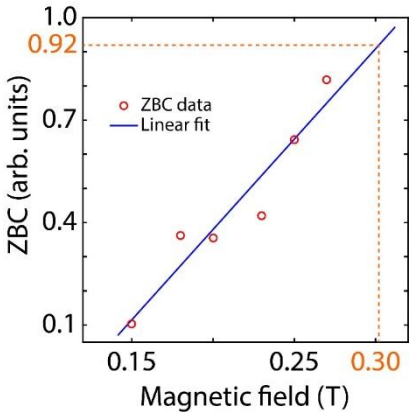

Figure S5. ZBC values as a function of magnetic field. ZBC values are extracted from the dI/dV spectra taken from the off-vortices regions. The upper critical field ~ 0.3 T is estimated by a linear fit.

6. Transition temperature (T_c)

Figure S6a-f demonstrate the fitting results of the spectra in Figure 3c. The gap size is obtained based on Dynes model[3] in each temperature (the 400 mK spectrum as well as its fitting curve has been shown in the main text Figure 1c. The gap size as a function of temperature is shown in Figure S6g. The fitting curve by BCS theory suggests that the T_c is 7.16 K, lower than that of bulk Pb. The fitting curve at low temperature obviously deviates from the data. The origin for the deviation is that the measured gap could be contributed by both superconducting gap and Coulomb gap, which provides more impact at low temperature. If the data points taken at 400 mK and 1.8 K are excluded, the fitting curve is more reliable (see Figure S6h). The corresponding T_c is 7.31 K, which is still not significantly higher than that of bulk Pb.

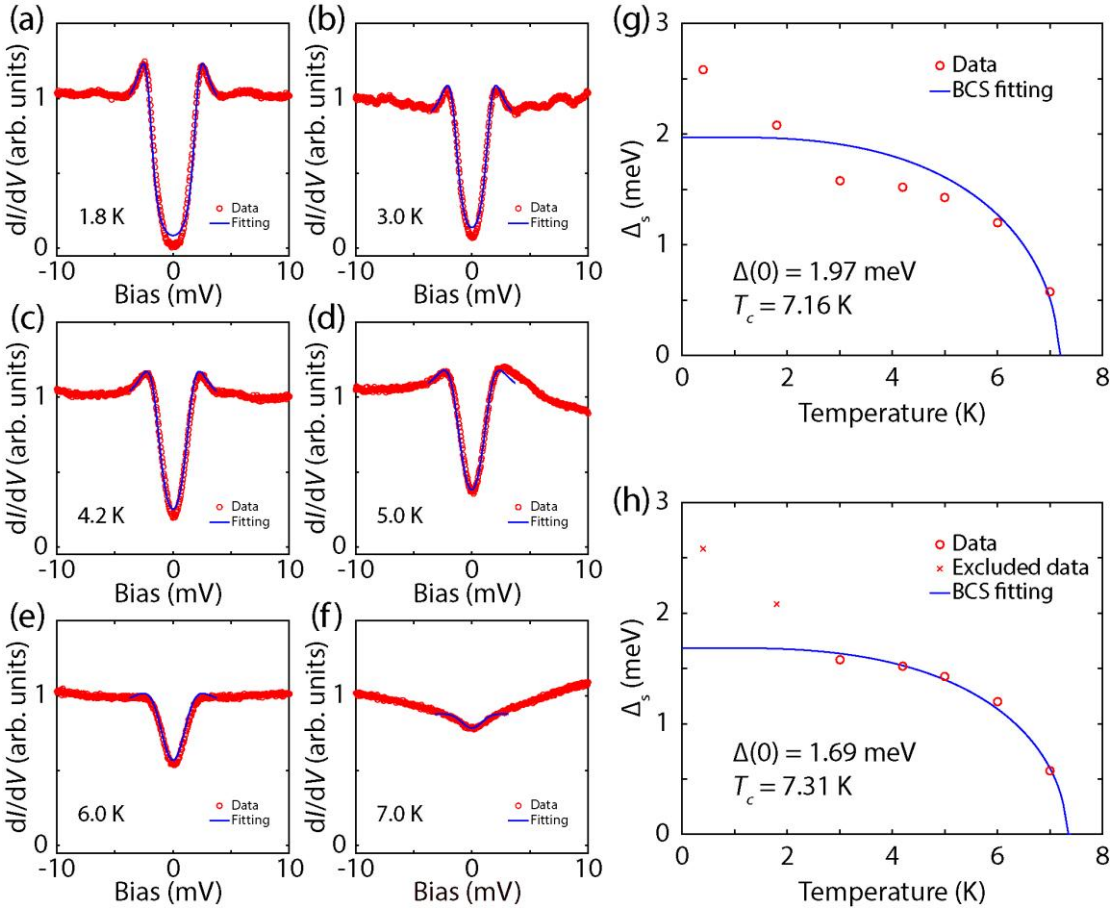

Figure S6. Estimation of transition temperature. (a-f) d*I*/d*V* spectra and fitting curves of the *R* = 30.8 nm Pb island at various temperatures. The data points are taken from the spectra in Figure 3c and denoted by red circles. The blues curves are the fitting results by Dynes model. (g) Superconducting gap size as a function of temperature. The red circles denote the gap size and the blue curve shows the fitting result by BCS theory. It suggests that the transition temperature T_c is 7.16 K. (h) The fitting result with same method but exclude the two data points at 400 mK and 1.8 K. The corresponding T_c is 7.31 K.

References

[1] Bose S et al. 2010 *Nat. Mater.* **9** 550
[2] Efros A and Shklovskii B 1975 *J. Phys. C: Solid State Phys.* **8** L49
[3] Dynes R C et al. 1978 *Phys. Rev. Lett.* **41** 1509